

CARBOPHANES: A NEW FAMILY OF CRYSTALLINE PHASES OF CARBON

R. H. Baughman and W. B. Hammond
Allied-Signal, Inc.
Research and Technology
Morristown, NJ 07962-1021

Keywords: Carbyne Carbon Phases, Carbophane Carbon Phases, Graphite Phase Transformation

I. Introduction:

This work is part of a continuing effort to develop structure-property predictions for new phases of carbon which are stable either at ambient or at high pressures [1]. The motivation is both to guide synthetic efforts to produce new carbon phases and to provide models for interpreting data for carbon phases of unknown structures.

Carbon crystals in which carbon exists in more than one hybridization state are the subject of the present analysis. Such materials are in sharp contrast with all available crystalline carbon phases with known structures, which contain either all sp^3 carbons (cubic diamond and Lonsdalite) or all sp^2 carbons (hexagonal graphite, rhombohedral graphite, and the newly discovered fullerenes). As is true for organic chemistry, the chemistry and physics of pure carbon is enormously expanded when one considers structures in which carbon is in more than one hybridization state. We have previously predicted structure-property relationships for a high thermal stability carbon phase which contains a mixture of sp^2 and sp carbon atoms [1]. This carbon phase, called graphyne, is presently the target of synthetic effort. Also, various high energy carbon phases have been proposed [2-7]. While carbon is known to exist in forms containing mixed states of carbon hybridization, all such well established forms are largely amorphous.

The family of carbon phases which we have constructed are called carbophanes, because of the similarities to the well known carbocyclic hydrocarbon molecules containing covalently bridged aromatic rings, which are called "phanes". These carbon phanes contain mixtures of sp^2 carbons, sp^3 carbons, and in some cases sp carbons. The structures and properties of these carbophanes will be compared with experimental results for (1) a phase or series of phases obtained by hydrostatic compression of graphite [8-14], (2) the crystalline transformation product obtained by rapid quenching of pulse-laser melted diamond [15], and (3) reported carbon phases which are often referred to in the literature as either "carbenes" or "carbynes" [16-19]. The structures are not established for any of these materials.

The high pressure transformation product of graphite which is of interest here was probably first discovered by Aust and Dickamer [8] in 1963, based on the observed increase in the resistivity of compressed graphite at about 15 GPa. However, the reported irreversibility of the phase change differs from the reversibility found in more recent work. Also, the reported x-ray data was later thought to originate from a contaminant [16]. Nevertheless, various investigators have firmly established the existence of a room temperature phase

transition for graphite which begins on increasing pressure to between 9 and 23 GPa. Upon decreasing the pressure to about 2 GPa or less, the new phase has been reported [11,12] to revert to a mixture of hexagonal and rhombohedral graphite. Electrical conductivity, optical reflectivity, and x-ray diffraction indicate that the high pressure phase is a crystalline insulator or a large bandgap semiconductor having low reflectivity between 1 and 3 eV [8-12]. This low reflectivity indicates that the interband absorption which occurs below 3 eV in graphite has been eliminated [10,13]. Also, the shear strength (determined by measuring pressure gradients and sample thickness in a diamond cell) is reported to exceed that of corundum and rhenium at 20 GPa, which is indicative of three-dimensional covalent bonding [11]. On the other hand, aromatic-like bonding is also suggested for the high pressure phase by Raman measurements at pressures between 38 and 55 GPa, which show a 100 cm^{-1} width peak centered at 1670 cm^{-1} [13]. However, other researchers report that the Raman spectrum could not be detected above 14 GPa [9]. Despite the width of this Raman line, the observation of at least three crystalline diffraction lines indicates that the transparent high pressure phase is not amorphous [11,12]. Structural models are herein proposed which provide electrical, optical and mechanical properties consistent with those observed. These carbophanes consist of covalently bonded sheets of carbon which contain aromatic rings that are isolated by sp^3 carbons. These structures are consistent with both the observed Raman line at about 1670 cm^{-1} , the low reflectivity between 1 and 3 eV, and the low conductivity. On the other hand, a high shear strength is provided by intersheet linkages via the sp^3 carbon atoms.

The experimental results reported for the carbyne phases are often contradictory and the initial structural assignment to linear chains of sp carbon atoms has added to the confusion [16-19]. There are several reasons why the above investigations are controversial. First, the reported properties of carbynes diverge from those predicted for chains of sp carbon atoms. These properties include, in specific instances, diamond-like hardness, a nonfibular morphology, colorless appearance, relatively high density, and high thermal and chemical stability. Second, atomic coordinates have not been provided which provide a satisfactory explanation for reported unit cell dimensions and diffraction intensities. This problem is understandable, since the derived unit cells are rather large and the only available diffraction data is either x-ray diffraction on polycrystalline and inhomogeneous material or electron diffraction data on very small crystallites which are in a matrix of another material. Third, it is not always clearly established that the investigated crystalline phase component contains only carbon. This problem is exaggerated for synthetic routes which are claimed to produce new carbon phases from organic polymer precursors. Moreover, most of the structural characterization is by electron diffraction, which can be misleading in that highly crystalline minority phase components due to impurities can be highlighted. In fact, Smith and Buseck [20] have assigned phase components attributed by others to carbon to a variety of non-carbonaceous phases. This assignment has been contested and it is presently difficult to decide which of the results reported in the literature is an artifact and which is correctly assigned to a new phase of carbon. The reported carbyne phases of interest here are hexagonal with unit cell parameter (a) in the basal plane in the range of 4.76 - 5.45 Å (or a factor of $\sqrt{3}$ higher) and an orthogonal cell dimension of either ~7.5, ~10, ~12.5, or ~15 Å [16-19]. The reasonable consistency of the a-axis dimension, as well as the systematic

variation in the c-axis dimension, suggest polytypic structures. These facts, as well as the continuing reports from diverse laboratories over three decades, suggests that the results are not all artifacts due to impurity components.

II. Description of Carbophane Polytypes:

The basic structural motif of the carbophanes is a covalently bonded layer having the same intralayer connectivity as graphite. In other words, carbon layers in the carbophanes consist of a two-dimensional array of six membered rings. However, in contrast with graphite, these layers in the benzenoid carbophanes consist of a mixture of sp^3 carbons in rings having the hybridization of 1,4-hexadiene and sp^2 carbons which are simultaneously in both these rings with the sp^3 carbons and in benzene rings. Transformation of 1/4 of the sp^2 carbons of graphite to sp^3 carbons, so that the remaining sp^2 carbons are all in benzene rings and no sp^3 carbons are adjacent in a layer, provides the benzenoid carbophanes. Each sp^3 carbon atom is covalently bonded within the layer to an sp^2 carbon in each of three benzene rings. The remaining covalent bond to each sp^3 carbon provides a covalent interlayer bond. In the case where the covalent bonds between layers are to the same neighboring layer, a bilayer structure results in which bonding between alternating layers is non-covalent. More interesting and diversified structures result when each layer containing the hexagonal rings is covalently bonded to two neighboring layers - thereby providing three-dimensionally covalently bonded structures in which there is one interlayer covalent bond to every fourth carbon atom in the hexagonal ring layer. Examples of the hydrocarbon cyclophanes, which are structurally related to the present carbophanes, are shown in Figure 1.

The carbophane phases are categorized according to the direction of intersheet sp^3 - sp^3 bonds for the fundamental structural motif, which is an aromatic ring surrounded by six sp^3 carbons (Figure 2). If a total of n sp^3 carbons bonded to a particular ring provide sp^3 - sp^3 bonds to the same neighboring sheet, a total of n indices denote the configuration of sp^3 - sp^3 bonds about this ring. These indices correspond to that of a ring carbon to which the associated sp^3 carbons are bonded. Correspondingly, there are seven motif isomers possible: 1,2,3,4,5,6-carbophane for $n = 6$; 1,2,3-carbophane, 1,3,5-carbophane, and 1,2,4-carbophane for $n = 3$; 1,2-carbophane, 1,3-carbophane, and 1,4-carbophane for $n = 2$; and 1-carbophane for $n = 1$. An example of a hexagonal ring sheet formed using the 1,3,5-carbophane motif is shown in Figure 2.

It is easily shown that the 1,2-, 1,4-, 1,2,3-, and 1,2,4-carbophane structures are unique. By unique we mean that there is only one way to covalently interconnect these motifs in a single motif structure. Also, the 1,3,5-carbophane has a type of uniqueness, since there is only one possible way to covalently interconnect the 1,3,5 motif, so as to provide the hexagonal ring sheet. However, these hexagonal sheets can be covalently interconnected with a neighboring sheet in two different ways, one which results in eclipsed aromatic rings, and one which results in non-eclipsed aromatic rings. These structures are named eclipsed 1,3,5-carbophane (or e-1,3,5-carbophane) and staggered 1,3,5-carbophane (or s-1,3,5-carbophane), respectively. Various mixtures of eclipsed and staggered sheets can be used to construct an infinite variety of either ordered or disordered forms of 1,3,5-carbophane which

contain basically the same structure for each hexagonal ring sheet. The structures for e-1,3,5- and s-1,3,5-carbophane viewed parallel to the molecular plane are shown in Figures 3 and 4, respectively.

In contrast with these types of uniqueness, there are an infinite number of possible ways (both periodic and non-periodic) to form covalent connections within the ring sheets using exclusively either the 1,3-carbophane or the 1-carbophane motif. Of the single motif structures, a structure with staggered (i.e. non-eclipsed) aromatic rings is possible only for 1,3,5-carbophane and 1-carbophane. Such structures are of special importance because of decreased strain energy compared with the corresponding fully eclipsed structures. As will be described elsewhere, partially staggered structures can arise for carbophanes having mixed motifs, such as an array of 1,3 and 1,3,5 motifs, where every layer can be either eclipsed on both sides or staggered on one side and eclipsed on the other. Note also that only the 1,3,5-carbophane and 1-carbophane structure could transform to diamond without the breaking of already formed covalent bonds. In such a manner, e-1,3,5-carbophane could transform to hexagonal diamond (Lonsdälite) and s-1,3,5-carbophane could transform to cubic diamond. All of the other above mentioned benzenoid carbophanes could transform to a fully sp^3 structure without bond breaking only by formation of energetically unfavorable cyclobutane rings.

There is another type of single-motif benzenoid carbophane structure which is possible, but this structure (which is analogous to the organic "superphane" shown in Figure 1) does not provide a three dimensionally covalently bonded structure. In this structure, which is denoted 1,2,3,4,5,6-carbophane, all intersheet sp^3 - sp^3 bonds from one sheet are connected to the same neighboring hexagonal ring sheet. These bilayers are bound with neighboring bilayers on either side by exclusively non-covalent interactions. Correspondingly, sheets of normal graphite planes could interdisperse with the bilayers, so as to provide an infinite variety of polytypic structures. From the viewpoint of close-packing, such polytypic structures would be expected to be thermodynamically unstable with respect to phase separation of the graphite sheets to make a pure graphite phase. However, such phase separation would be extremely unfavorable, kinetically.

III. Calculation of Crystal Structures and Strain Energies:

We have used the crystal building capabilities of the software program PolyGraf [21] and a modified Dreiding force field [22] to generate energy minimized unit cell parameters and atom coordinates for the simplest members of the carbophane family of phases. The Dreiding force field was modified to reproduce the known structures for a series of organic cyclophanes [27-29] shown in Figure 1. Note that the present force field provides sp^2 - sp^2 bond lengths and force constants appropriate for an isolated aromatic ring, as in a benzenoid carbophane (with a π -bonding order of 1/2 per bond). Consequently, the intralayer bond distances which are predicted for graphite are too short (the π -bond order in graphite is 1/3) and the calculated density of graphite is correspondingly too high, although the graphite interlayer distance is correctly predicted by our force field. The present calculation does not take into account changes in π -bond order in the aromatic rings due to ring distortion, which might provide contributions from quinoid-like structures.

The present crystal structure calculations for carbophane phases provide enthalpies (H_1) relative to a hypothetical reference state in which the terms in the calculation Hamiltonian are zero. The standard heat of formation of a carbophane is obtained by adding the above energy H_1 (which is largely a strain energy) to the energy of the reference state for a carbophane (relative to graphite), which is denoted H_0 . H_0 is calculated using experimentally derived heats of formation of model hydrocarbon molecules which contain an sp^3 carbon atom covalently bonded to three sp^2 carbon atoms in benzene rings and to an sp^3 carbon, as in carbophane. This is done by first using the molecular mechanics force field to calculate the strain energies (H_1) for the model compounds. Using this strain energy and the experimentally derived gas phase heats of formation, $H_f(g)$, for a model compound, H_0 for the model compound becomes $H_0 = H_f(g) - H_1 - 4RT$, where the term $4RT$ corrects for the enthalpy contributions due to rotational and translational motion ($3RT$) and the difference between constant volume and constant pressure gas phase heat capacities (RT).

Using this approach, H_0 for the family of carbophanes was calculated as follows: $H_0(\text{carbophane}) = 1/4 H_0(1,1,1\text{-triphenylethane}) - 1/8 H_0(\text{ethane}) - 5/8 H_0(\text{benzene})$. Using gas phase formation enthalpies for these hydrocarbons reported in the literature [30,31], the resulting value of H_0 for the reference state of a benzenoid carbophane is 0.85 kcal/mole carbon.

If we approximate the effective bond energy of an sp^2 - sp^3 bond as the average of sp^2 - sp^2 and sp^3 - sp^3 bonds, a second estimate for H_0 of benzenoid carbophane can be obtained from the heat of formation of diamond [32] and the gas phase heats of formation of benzene and biphenyl [31]. The equation for H_0 of carbophane is then: $H_0(\text{carbophane}) = 3/8 H_0(\text{biphenyl}) - 5/8 H_0(\text{benzene}) + H_0(\text{diamond})$. The resulting value of H_0 is -0.94 kcal/mole carbon, which is somewhat lower than the above value of +0.85 kcal/mole carbon. Which value is more reliable cannot presently be determined, since the former calculation contains an uncertainty due to the required estimation of the heat of sublimation of the triphenylethane [30], using group increments, and the latter value is uncertain because of the above bond-energy approximation. Although these values of H_0 are both close to zero, the uncertainties in H_0 limit our ability to calculate equilibrium transition pressures for the interconversion between graphite and the carbophanes.

IV. Properties Evaluation:

Based on experimental observations for multilayered organic benzenoid cyclophanes, the present benzenoid carbophanes are expected to be colorless. For example, Otsubo et al. [33] investigated the effect of layer number on the optical properties of [2.2]paracyclophanes having from 2 to 6 layers. The two layer form of this compound is shown in Figure 1. With increasing layer number, strong bathochromic and hyperchromic changes are observed in the ultraviolet absorption spectra. However, these effects rapidly saturate, so that little change is observed in going from a five layer to a six layer [2.2]paracyclophane, both of which form colorless crystals. Similarly, both fluorescence and phosphorescence spectra exhibit large bathochromic shifts

and the phosphorescence lifetime decreases with increasing layer number. Also, the charge-transfer complexes with acceptors, such as tetracyanoethylene or trinitrobenzene, demonstrate bathochromic shifts of the long wavelength charge-transfer band and an increased association constant for increasing numbers of layers in the paracyclophanes. These shifts in optical properties with increasing number of layers, which are close to saturation for six layer [2.2]cyclophane, largely arise from interlayer π -electron interactions between neighboring aromatic rings. Based on the similar optical properties of unsubstituted cyclophanes and cyclophanes with severe aromatic ring distortions due to eclipsed methyl substituents (as well as the absence of large shifts in the absorption curves for [m]cyclophanes having aromatic ring strain similar to the [2.2]paracyclophanes [34]), the optical property changes due to aromatic ring distortions are expected to be relatively unimportant [33].

The above observations on the multilayered organic benzenoid cyclophanes also suggest that the corresponding eclipsed benzenoid carbophanes with three-dimensional covalent bonding will display red shifts in absorption, fluorescence, and phosphorescence spectra (and a decrease in phosphorescence lifetimes) with decreasing interlayer separation, due to increased π -electron interactions in the stacks of aromatic rings. The decreased phosphorescence lifetime is expected to be a result of a lowering of the energy gap between ground and triplet states as a result of increasing interactions between benzene rings. More specifically, using observations on the stacked [2.2]paracyclophanes [33], an absorption onset at about 3.3 eV, a fluorescence maxima at about 390 nm, and a phosphorescence maxima at about 530-570 nm are expected for an eclipsed carbophane having a spacing between aromatic ring carbons of about 2.97 Å. Such spacings are in the range predicted for carbophanes. A blue shift in these spectra and an increased phosphorescence lifetime is expected for the eclipsed carbophanes in Table 1 having longer interlayer separations, while those eclipsed carbophanes having shorter interlayer separations are expected to behave in the opposite manner. Pressure will decrease the interlayer spacing and produce the corresponding effects on the electronic states.

Note that the calculated densities for the carbophanes in Table 1 range from 2.479 g/cm³ for s-1-carbophane to 2.801 g/cm³ for e-1,3,5-carbophane. The calculated densities of these phases are intermediate between those of hexagonal graphite ($\rho(\text{obs.})=2.267$ g/cm³) and diamond ($\rho(\text{obs.})=3.52$ g/cm³ and $\rho(\text{calc.})=3.502$ g/cm³). Excluding the highest density phases (e-1,3,5-carbophane and s-1,3,5-carbophane), the calculated strain energies of the carbophanes are represented within a maximum deviation of 0.24 kcal/mole by a linear dependence on calculated density ($H_1 = -20.32 + 9.26 \rho$). Staggered 1,3,5-carbophane has a 0.56 kcal/mole lower strain energy and eclipsed 1,3,5-carbophane has a 0.65 kcal/mole higher strain energy than provided by this linear correlation. Consequently, the s-1,3,5-carbophane phase is especially interesting as a phase which might be thermodynamically stable with respect to graphite at high pressure. Note that this phase shows a large density increase with respect to the density of graphite, while requiring a smaller than expected formation energy with respect to graphite at zero pressure. Although increasing the temperature will decrease the formation free energy of a carbophane relative to diamond, because of entropy contributions, diamond will

have a lower free energy than any carbophane phase at room temperature and any pressure.

Calculated bulk moduli for carbophanes and for diamond are also listed in Table 1. Using the modified Dreiding force field, a bulk modulus of 477 GPa is obtained for diamond, as compared with a measured value of 442 GPa [35]. Staggered-1,3,5-carbophane has the highest calculated bulk modulus and the highest bulk density of all the benzenoid carbophanes studied. The bulk modulus of s-1,3,5-carbophane is 240 GPa, which is 54% of the observed modulus of diamond and 7.1 times the observed [9] bulk modulus of graphite (33.8 GPa). Since 1,2,3,4,5,6-carbophane does not have three-dimensional covalent bonding, but instead consists of bilayers which are connected to neighboring bilayers by exclusively non-covalent bonding, a bulk modulus of about twice that of graphite is expected for this phase. Consistent with this view, the ratio of the calculated bulk modulus for 1,2,3,4,5,6-carbophane to the observed bulk modulus for graphite is 2.2.

V. Conclusions:

A carbophane phase provides an interesting model for the room temperature, high pressure transformation product of graphite (HP phase). A number of points provide support for such a model. First, the HP phase is reported to revert to a mixture of hexagonal and rhombohedral graphite upon a reduction in pressure at room temperature [11-12], which would appear to exclude assignment as a polytype of diamond. While the carbophanes are expected to have a considerable degree of kinetic stability at zero pressure, defects (due to imperfect phase transformation, for the ambient temperature formation process) could propagate as molecular scale cracks upon the unloading of pressure, thereby facilitating the reconversion to graphite. Second, formation of carbophanes is expected to be kinetically favorable, since no covalent bond breaking is required to transform graphite to a carbophane and a lower degree of cooperative reaction is required than to form a diamond polytype. Third, eclipsed carbophanes are predicted to be transparent up to about 3.3 eV and staggered carbophanes are probably transparent to an even higher energy. This is consistent with the reported bleaching of the interband transition of graphite below 3 eV in going to the HP phase [10,13]. Fourth, the carbophanes would provide a Raman peak (corresponding to the aromatic ring mode) close to that observed for the HP phase, since the in-plane ring stretch occurs in the 1620-1565 cm^{-1} region at atmospheric pressure for various cyclophanes [36]. Fifth, the carbophanes, such as s-1,3,5-carbophane, are calculated to have a bulk modulus which is up to 50% that of diamond, consistent with the report that the HP phase is a superhard material with a strength comparable to diamond [11].

Regarding the possibility that carbophanes might have been already observed at ambient pressure, but unrecognized as such, it is interesting to note that Weathers and Bassett [15] have reported that new crystalline carbon phases are produced as microscopic components by pulsed-laser melting of diamond at high pressures in a diamond anvil cell. As the pressure during the laser pulse is increased from 10 to 30 GPa, the long diffraction spacing observed for the transformation product decreases from 3.4 Å, as in graphite, to 2.8 Å. As shown in Table 1, this is about the range of intersheet spacings which we have

derived for three-dimensional carbophane phases (from 3.17 Å for 1,2,3-carbophane to 2.72 Å for s-1,3,5-carbophane). Additionally, it is interesting to note that the carbophanes provide the diamond-like hardness, non-fibular morphology, colorless appearance, and relatively high density that researchers have attributed to the mysterious carbyne phases [16-19]. Also, if these phases are well ordered, they could provide the high thermal and chemical stability which has been claimed for the carbynes. The directly bridged carbophanes described herein do not provide the acetylenic bond, which is the claimed component of carbynes [16-19]. The evidence for such bonds in the crystalline phase is not firmly established, because of the possibility that the spectroscopic signature for their type of bonding is from the matrix. Nevertheless, acetylene-containing polytypes can be readily constructed from the present carbophane phases by replacing sp^3 - sp^3 interlayer bridges with sp^3 - $sp \equiv sp$ - sp^3 linkages for either a fraction or for all of the interlayer separations. We have shown that the resulting unit cell parameters reproduce reasonably well those in the literature of carbynes [16-19].

This is an interim report of continuing work on what we believe to be an important family of new carbon phases. Work in progress will extend the carbophane family of phases to mixed motif and disordered variants, refine and extend property predictions, and provide comprehensive comparisons of predicted properties with those reported in the substantial literature which claims new crystalline carbon phases. It will also be interesting to see whether or not the fundamental packing arrangements in the carbophanes provide a useful framework for structural models of "amorphous" diamond-like carbon. These materials are known to consist of mixtures of sp^3 and sp^2 hybridized carbons.

References

1. R. H. Baughman, H. Eckhardt, and M. Kertesz, *J. Chem. Phys.* **87**, 6687 (1987).
2. M. T. Yin and M. L. Cohen, *Phys. Rev. Lett.* **50**, 2006 (1983).
3. K. M. Merz, R. Hoffmann, and A. T. Balaban, *J. Am. Chem. Soc.* **109**, 6742 (1987).
4. G. Laqua, H. Musso, W. Boland, and R. Aldrichs, *J. Am. Chem. Soc.* **112**, 7391 (1990).
5. M. A. Tamor and K. C. Hass, *J. Mater. Res.* **5**, 2273 (1990).
6. A. T. Balaban, C. C. Rentia, and E. Ciupitu, *Revue Roumaine de Chimie* **13**, 231 (1968).
7. R. Hoffman, T. Hughbanks, M. Kertesz, and P. H. Bird, *J. Am. Chem. Soc.* **105**, 4832 (1983).
8. R. B. Aust and H. G. Drickamer, *Science* **140**, 817 (1963).
9. M. Hanfland, H. Beister, and K. Syassen, *Phys. Rev. B* **39**, 12598 (1989).
10. M. Hanfland, K. Syassen, and R. Sonnenschein, *Phys. Rev. B* **40**, 1951 (1989).
11. J. F. Shu, H. K. Mao, J. Z. Hu, Y. Wu, and R. J. Hemley, *Bull. Am. Phys. Soc.* **36**, 479 (1991).
12. Y. X. Zhao and I. L. Spain, *Phys. Rev. B* **40**, 993 (1989).
13. A. F. Goncharov, I. M. Makarenko, and S. M. Stishov, *High Pressure Research* **4**, 345 (1990).
14. A. A. Goncharov, *Zh. Eksp. Teor. Fiz.* **98**, 1824 (1990).

15. M. S. Weathers and W. A. Bassett, *Phys. Chem. Minerals* **15**, 105 (1987).
16. L. I. Man, Y. A. Malinovskii, and S. A. Semiletov, *Sov. Phys. Crystallogr.* **35**, 608 (1990).
17. A. G. Whittaker and P. L. Kintner, *Science* **165**, 589 (1969).
18. R. B. Heimann, J. Kleiman, and N. M. Salansky, *Carbon* **22**, 147 (1984).
19. A. M. Sladkov, *Soviet Sci. Rev. Sec. 3*, 75 (1981).
20. P. K. Smith and P. R. Buseck, *Science* **216**, 986 (1982).
21. PolyGraf is an interactive molecular simulation/three-dimensional graphics program from Molecular Simulations, Inc., Sunnyvale, CA, 94086
22. The following adjustments were made in the Dreiding force field [23]. The van der Waals interactions were treated with an exponential-six potential with parameters for hydrogen ($R_0=3.1665 \text{ \AA}$, $D_0=0.0200 \text{ kcal/mole}$, and $\zeta=11.2$) and carbon ($R_0=3.8410 \text{ \AA}$, $D_0=0.07918 \text{ kcal/mole}$, and $\zeta=13.0$) [24]. A Morse potential was used for bond stretching with $B_0(\text{sp}^3\text{-sp}^3)=1.525 \text{ \AA}$, $B_0(\text{sp}^3\text{-sp}^2)=1.500 \text{ \AA}$, and $B_0(\text{sp}^2\text{-sp}^2)=1.375 \text{ \AA}$. A theta expansion was used for the angle bending term with $\Theta_0(\text{sp}^3\text{-sp}^3\text{-sp}^2)=112.0^\circ$. The Dreiding force field uses a six-fold torsion term with a barrier height of 1.0 kcal/mol. and a cis max for rotation about an sp^3 carbon bonded to an aromatic ring. We were better able to reproduce the barriers for rotations reported by Schaefer et al. for ethylbenzene [25] and isopropylbenzene [26] if this term was set equal to zero.
23. S. L. Mayo, B. D. Olafson, and W. A. Goddard, III, *J. Phys. Chem.* **94**, 8897 (1990).
24. N. Karasawa, S. Dasgupta, and W. A. Goddard, III, *J. Phys. Chem.* **95**, 2260 (1991).
25. T. Schaefer, G. Penner, and R. Sebastian, *Can. J. Chem.* **64**, 873 (1986).
26. T. Schaefer, R. Sebastian, and G. Penner, *Can. J. Chem.* **66**, 1945 (1988).
27. H. Hope, J. Bernstein, and K. N. Trueblood, *Acta Cryst.* **B28**, 1733 (1972).
28. A. W. Hanson, *Cryst. Struct. Comm.* **9**, 1243 (1980).
29. A. W. Hanson and T. S. Cameron, *J. Chem. Research (S)* 336 (1980).
30. R. M. Joshi, *J. Macromol. Sci., Chem.* **A5**, 687 (1971).
31. D. R. Stull, E. F. Westrum, Jr., and G. C. Sinke, *The Chemical Thermodynamics of Organic Compounds*, Sec. III, pp. 631-769 (Wiley, New York, 1969).
32. P. Hawtin, J. B. Lewis, N. Moul, and R. H. Phillips, *Proc. Soc. London A* **261**, 67 (1966).
33. T. Otsubo, S. Mizogami, I. Otsubo, Z. Tozuka, A. Sakagami, Y. Sakata, and S. Misumi, *Bull. Chem. Soc. Jap.* **46**, 3519 (1973).
34. N. L. Allinger, L. A. Freiberg, R. B. Hermann, and M. A. Miller, *J. Am. Chem. Soc.* **85**, 1171 (1963).
35. M. H. Grimsditch and A. K. Ramdas, *Phys. Rev. B* **11**, 3179 (1975).
36. P. H. Scudder, V. Boekelheide, D. Cornutt, and H. Hopf, *Spectrochimica Acta* **37A**, 425 (1981).

Table 1. Calculated Structural Features of Carbon Phases

Carbon Phase	Space Group	Density g/cm ³	Z ^a	H ₁ (strain) (kcal/mol)	Interlayer Spacing, Å	Bulk Modulus (GPa)
s-1-carbophane	P $\bar{3}1m$	2.479	48	2.398	3.074	101
e-1-carbophane	P $\bar{6}2m$	2.672	48	4.345	2.926	135
	Cmcm	2.672	64	4.367	2.924	129
1,2-carbophane	Cmcm	2.547	64	3.376	3.125	109
1,3-carbophane	Cmcm	2.737	64	5.128	2.853	192
	P $\bar{6}2m$	2.733	48	5.104	2.858	191
1,4-carbophane	Immm	2.722	32	4.862	2.884	199
1,2,3-carbophane	Imma	2.514	32	3.205	3.169	106
1,2,4-carbophane	Cmca	2.707	64	4.573	2.903	195
s-1,3,5-carbophane	R $\bar{3}m$	2.840	24	5.418	2.724	240
e-1,3,5-carbophane	P $\bar{6}_3/mmc$	2.801	16	6.271	2.775	238
1,2,3,4,5,6-carbophane	P6/mmm	2.636	16	4.190	2.672 ^b	75
					3.226 ^c	
graphite	P $\bar{6}_3mmc$	2.405	4	-0.007	3.355	43
	R $\bar{3}m$	2.402	2	0.010	3.355	
diamond	Fd $\bar{3}m$	3.502	8	0.992	2.059 ^d	477
	P $\bar{6}_3/mmc$	3.490	4	2.591	2.180 ^e	473

^a Atoms per unit cell. ^b Distance between covalently bonded layers. ^c Distance between van der Waals bonded layers. ^d (111) spacing. ^e (100) spacing.

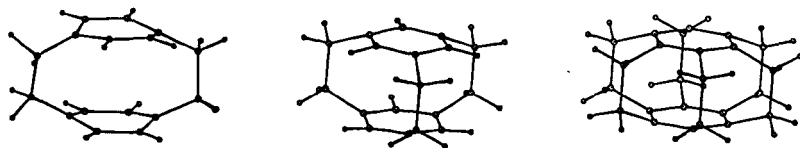


Figure 1. Organic cyclophanes which contain the intersheet bonding arrangement of 1,4-carbophane, 1,3,5-carbophane, and 1,2,3,4,5,6-carbophane.

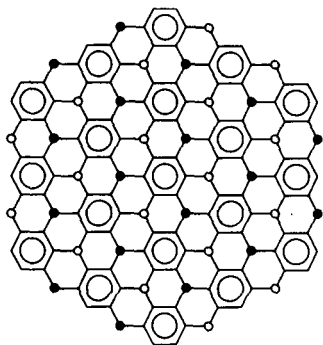


Figure 2. The bonding arrangement for e and s-1,3,5-carbophane showing the six sp^3 carbons surrounding each aromatic ring. Open and closed circles indicate sp^3 bonding below and above the layer plane, respectively.

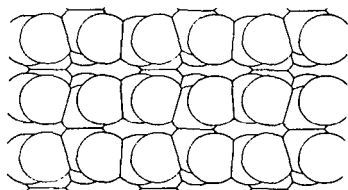


Figure 3. The crystal structure for e-1,3,5-carbophane viewed normal to the intersheet sp^3-sp^3 bond and parallel to the sheet plane.

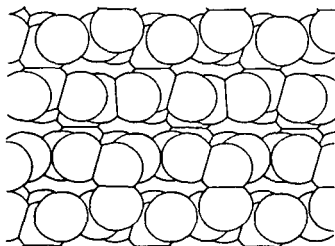


Figure 4. The crystal structure for s-1,3,5-carbophane viewed normal to the intersheet sp^3-sp^3 bond and parallel to the sheet plane.